

Cell-penetrating chitosan/doxorubicin/TAT conjugates for efficient cancer therapy

Jue-Yeon Lee^{1,2}, Young-Suk Choi^{1,2}, Jin-Sook Suh^{1,2}, Young-Min Kwon³, Victor C. Yang³, Seung-Jin Lee⁴, Chong-Pyoung Chung^{2,5} and Yoon-Jeong Park^{1,2}

¹ Department of Craniomaxillofacial Reconstructive Science, School of Dentistry, Seoul National University, Seoul, Korea

² Intellectual Biointerface Engineering Center, College of Dentistry, Seoul National University, Seoul, Korea

³ Department of Pharmaceutical Sciences, College of Pharmacy, University of Michigan, Ann Arbor, Michigan, USA

⁴ Department of Pharmacy, College of Pharmacy, Ewha Womans University, Seoul, South Korea

⁵ Department of Periodontology, School of Dentistry, Seoul National University, Seoul, Korea

In this study, a cell-penetrating peptide, the transactivating transcriptional factor (TAT) domain from HIV, was linked to a chitosan/doxorubicin (chitosan/DOX) conjugate to form a chitosan/DOX/TAT hybrid. The synthesized chitosan/DOX/TAT conjugate showed a different intracellular distribution pattern from a conjugate without TAT. Unlike both free DOX and the conjugate without TAT, the chitosan/DOX/TAT conjugate was capable of efficient cell entry. The chitosan/DOX/TAT conjugate was found to be highly cytotoxic, with an IC₅₀ value of approximately 480 nM, 2 times less than that of chitosan/DOX (980 nM). The chitosan/DOX/TAT provided decreases in tumor volume of 77.4 and 57.5% compared to free DOX and chitosan/DOX, respectively, in tumor-bearing mice. Therefore, this study suggests that TAT-mediated chitosan/DOX conjugate delivery is effective in slowing tumor growth.

Water soluble polymers, including *N*-(2-hydroxypropyl)-methacrylamide (HPMA) copolymers^{1,2} and polysaccharides such as cyclodextrin,³ are frequently applied as drug carriers as they have the ability to improve the solubility of hydrophobic compounds. This in turn increases the therapeutic index of low-molecular-weight drugs by raising drug payloads

per molecule of polymer, improves the stability of conjugated drug molecules⁴ and enhances the drug's tumor retention capability, known as the EPR effect.⁵ Over the past two decades, the concept of using water-soluble polymers as drug carriers has been proposed and validated by several research groups, including Kopecek *et al.*⁴ and Duncan.⁶ The intracellular delivery of polymeric drug carriers, however, has been a challenge due to their large size and inherently poor penetration capabilities. Furthermore, the endocytotic or phagocytic uptake characteristic of such macromolecules directs these polymers to the endosomes, where they are susceptible to enzymatic and acidic degradation. Recently, a series of peptides named protein transduction domain (PTD) peptides,⁷⁻⁹ such as the peptide from the transactivating transcriptional factor (TAT) protein of HIV, have been discovered and extensively investigated. PTDs can translocate across almost all types of eukaryotic plasma membranes through a seemingly energy-independent pathway. In addition, following chemical hybridization to other macromolecules or even nanoparticulates, PTDs can transduce these linked species into cells and tissues and even cross the blood-brain barrier (BBB), a highly impermeable barrier in the body.⁹ The BBB comprises endothelial cells of the brain tissue capillaries. The endothelial cells are connected by tight junctions and form an epithelial-like, high-resistance barrier.¹⁰ Our previous reports also demonstrated that the PTD peptide successfully delivered protein molecules into cells *in vitro* and *in vivo*, thereby enhancing diagnostic or therapeutic activity compared with proteins not hybridized to the PTD.¹¹⁻¹³ The objective of this research was to examine whether PTDs (in particular TAT) could improve the intracellular localization of polymeric drugs

Key words: Cell-penetrating peptide, TAT, chitosan conjugate, doxorubicin, tumor

Abbreviations: BBB: blood-brain barrier; DOX: doxorubicin; EDTA: ethylenediamine tetraacetic acid; EPR: enhanced permeability and retention; FACS: fluorescence activated cell sorter; FBS: fetal bovine serum; FPLC: fast protein liquid chromatography; HIV: human immunodeficiency virus; HPMA: *N*-(2-hydroxypropyl)-methacrylamide; MDR: multidrug resistance; MTT: 3-(4: 5-dimethylthiazol-2-yl)-2: 5-diphenyl tetrazolium bromide; PBS: phosphate buffered saline; PTD: protein transduction domain; SATP: *N*-succinimidyl *S*-acetylthiopropionate; SMCC: succinimidyl 4-(*N*-maleimidomethyl) cyclohexane-1-carboxylate; TAT: transactivating transcriptional factor

Grant sponsors: Korea Healthcare technology R&D project, Ministry for Health, Welfare & Family Affairs, Republic of Korea;

Grant number: A080927

DOI: 10.1002/ijc.25578

History: Received 28 May 2010; Accepted 21 Jul 2010; Online 28 Jul 2010

Correspondence to: Yoon-Jeong Park, Department of Craniomaxillofacial Reconstructive Science, School of Dentistry, Seoul National University, Seoul, Korea, Tel: 82-2-740-8651, Fax: 82-2-744-8732, E-mail: parkyj@snu.ac.kr

composed of chitosan and doxorubicin (DOX). Chitosan is the *N*-deacetylated derivative of chitin and has been utilized as a drug^{14,15} or gene carrier^{16–18} due to its biomedical advantages, including biocompatibility and biological activity. In addition, the reactive amino groups in the backbone of chitosan make it possible to chemically conjugate various biological molecules, such as growth factor and antibody.^{19,20} DOX has been used as the drug of choice in cancer therapy but has produced undesirable side effects, such as cardiotoxicity, due to a wide tissue distribution, including the heart.²¹ Therefore, DOX incorporation into polymeric drug carriers, such as nanoparticles^{22,23} or micellar carriers,^{24,25} has been attempted in experimental cancer therapies. However, non-specific drug leakage from the carrier also evokes side effects; thus, direct conjugation to the carrier has been alternatively attempted. Mitra *et al.*²² attempted DOX and dextran coupling and then encapsulated the DOX-dextran conjugate in chitosan hydrogel nanoparticles to reduce the side effects of DOX.

The direct conjugation between chitosan and DOX has not yet been attempted in other studies. Although the polymeric anticancer drug conjugates can create an enhanced permeability and retention (EPR) effect in the tumor, they have limited tumor localization activity. In this study, a PTD was introduced into chitosan/DOX conjugates to achieve increased tumor penetration by the PTD and to create enhanced tumor localization of the polymeric drug conjugate. A sulfhydryl group was introduced to the amine moieties in chitosan, and then, DOX was conjugated via SMCC to chitosan. Finally, TAT was conjugated to chitosan/DOX *via* the formation of a disulfide bond. In this report, we describe the synthesis of chitosan/DOX/TAT conjugates, their internalization into cells and the antitumor activity of the conjugates *in vitro* and *in vivo*.

Material and Methods

Materials

Chitosan was purchased from Fluka (St. Louis, MO). Doxorubicin and MTT were purchased from Sigma Aldrich (St. Louis, MO). Fetal bovine serum (FBS), phosphate-buffered saline (PBS), 0.25% (wt/vol) trypsin-EDTA, RPMI-1640 medium, Dulbecco's Modified Essential Medium (DMEM), α -Minimum Essential Medium (α -MEM) and penicillin/streptomycin antibiotics were from Gibco-BRL (Gaithersburg, MD). *N*-succinimidyl-S-acetylthiopropionate (SATP) and the bifunctional cross-linkers, 1-ethyl-3-(3-dimethylaminopropyl) carbodiimide hydrochloride (EDC) and *N*-succinimidyl-3-(2-pyridylidithio) propionate (SPDP), were obtained from Pierce (Rockford, IL). CT-26 adenocarcinoma cells were obtained from the American Type Culture Collection (Manassas, VA). The PTD TAT (CGGGYGRKKRRQRRR) was chemically synthesized using an automatic peptide synthesizer based on F-moc chemistry. The prepared peptide was further purified using HPLC. The underlined sequence of the TAT peptide is

the core sequence of the peptide responsible for membrane transduction. Another four amino acid residues were added at the *N*-terminus of the peptide to introduce a sulfhydryl (-SH) group (cysteine) for conjugation to chitosan and to enhance the flexibility of the peptide (GGG sequence). All other chemicals used were of analytical grade.

Synthesis of chitosan/DOX/TAT conjugates

Chitosan solution [m.w. 2000, 1 mg/mL in PBS (pH 7.4, 1.05 mM KH₂PO₄, 155 mM NaCl and 2.9 mM Na₂HPO₄•7H₂O)] was allowed to react with *N*-succinimidyl S-acetylthiopropionate (SATP, 50 mM in PBS; Pierce) and was then reacted with 50 mM hydroxylamine solution (10 mM EDTA in PBS) to generate the sulfhydryl group in chitosan. The unreacted SATP was removed by ultrafiltration using a 1.0-K molecular weight cutoff membrane. The sulfhydryl content was assayed using Ellman's Reagent (Pierce) according to the manufacturer's instructions. The chitosan/DOX conjugate was generated by linking the sulfhydryl groups in chitosan and DOX with a heterobifunctional crosslinker, succinimidyl 4-(*N*-maleimidomethyl) cyclohexane-1-carboxylate (SMCC; 50 mM in PBS; Pierce). A volume of 20 μ L of triethylamine and 300 μ L of SMCC (18 mg/ml in DMSO) were added to the DOX solution (0.2 mg/mL in PBS, pH 8). The mixture was incubated at room temperature for 2 h. After adjusting the pH of the mixture to 5.5, 2 mL of sulfhydryl chitosan solution was added (1.5 mg/mL in PBS). The mixture was incubated at room temperature for 2 h and then kept at 4°C overnight. The free DOX, SMCC and triethylamine were removed from the chitosan/DOX solution *via* ultrafiltration using a 1.0-K molecular weight cutoff membrane. After adjusting the pH of the chitosan/DOX solution to 5.5, the TAT peptide (1.0 mg/0.2 mL PBS) was added. The mixture was incubated at room temperature for 2 h and then kept at 4°C overnight. The chitosan/DOX/TAT conjugates were separated from free chitosan, chitosan/DOX and TAT by passing the mixture through a HiTrap heparin affinity column connected to a FPLC with a gradient elution containing a 2.0 M NaCl solution.²³ Elution profiles were determined by absorbance at 280 nm. The column was eluted at a flow rate of 1 mL/min, while the NaCl gradient was increased at a rate of 50 mM/min. Salts in the collected chitosan/DOX/TAT conjugate fraction were removed by passing the sample through a desalting column and washing with PBS. Successful production of the chitosan/DOX/TAT conjugate was confirmed by SDS-PAGE.

Flow cytometric analysis

The cells were seeded at a density of 1×10^6 cells per well in six-well plates in 1.5 mL culture medium. One day later, the cells were washed and incubated with DOX, chitosan/DOX or chitosan/DOX/TAT conjugates (0.2 μ M) for 30 min at 37°C in humidified 5% CO₂. To study cell internalization in the presence of serum, the peptides were dissolved in DMEM in the absence of serum, followed by the addition of 10% FBS. After incubation, cells were washed with PBS, treated

extensively with trypsin-EDTA to remove surface-bound conjugates and washed again. The cells were then fixed with 1% paraformaldehyde and washed with PBS. Analysis was conducted on a FACScaliber flow cytometer (Becton Dickinson, San Jose, CA) equipped with a 635-nm red dye laser. The fluorescence of 5,000 vital cells was acquired, and data were visualized in logarithmic mode.

Confocal microscopic observation of chitosan/DOX/TAT internalization

The cultivation of the CT-26 colon adenocarcinoma cell line was conducted as described previously.¹³ Cells were plated on Lab-Tek (4-well) chamber slides (Nalgene Nunc International, Naperville, IL) at a density of 1×10^4 cells/1.8 cm² and incubated at 37°C in a humidified 5% CO₂ atmosphere. After complete adhesion, the culture medium was removed. The chitosan/DOX conjugate or chitosan/DOX/TAT conjugate was then added to the cells at a final concentration of 0.2 μM. Following a 30-min incubation at 37°C in a humidified 5% CO₂ atmosphere, the cells were extensively washed and fixed in 1% (wt/vol) paraformaldehyde in PBS for 20 min at room temperature. Nuclear staining was conducted with Hoechst 33342 (5 μg/ml; Molecular Probes) according to the manufacturer's protocol. Coverslips were mounted onto slides using ProLong Gold (Molecular Probes). Confocal microscopy was carried out using an inverted LSM 510 laser scanning microscope (Carl Zeiss, Gottingen, Germany) equipped with a Plan-Apochromat 63×, 1.4 N.A. or 40×, 1.4 N.A. lens. The laser was set at 358 nm (blue) and 543 nm (orange) to produce the excitation wavelengths for DAPI and rhodamine, respectively. Z-series were taken of a 1- to 2-μm optical section at 2-μm intervals.

Cytotoxicity assay

Evaluation of the cytotoxicity of each conjugate was conducted using the MTT assay. In general, the CT-26 cells were seeded at a density of 1.0×10^4 cells/well in a 96-well flat-bottomed microassay plate (Falcon, Becton Dickinson, Franklin Lakes, NJ) and incubated for 24 h. Fluorescence intensity measurements of doxorubicin in the chitosan/DOX and chitosan/DOX/TAT conjugates, DOX/TAT and free DOX solutions were used to determine and adjust the drug concentrations. DOX/TAT conjugate was synthesized according to a previous report.¹¹ The conjugates were then added in varying concentrations to the culture media, and the mixture was incubated for another 72 h at 37°C. At the end of the experiment, the medium was replaced with 200 μL of fresh DMEM medium without serum, and 120 μL of 2 mg/ml MTT solution in PBS was added. After incubation for an additional 4 h at 37°C, the MTT-containing medium was removed, and 200 μL of dimethyl sulfoxide was added to dissolve the formazan crystals formed by the live cells. The absorbance of the solution in each well was measured by a microplate reader (Bio-Tek, Winooski, VT) at a wavelength of 540 nm. Cell

viability (%) was calculated according to the following equation:

$$\text{Cell viability (\%)} = \left(\frac{\text{absorbance of cells treated with each conjugate}}{\text{absorbance of cells not treated with each conjugate}} \right) \times 100.$$

In vivo distribution and antitumor effect of chitosan/DOX/TAT conjugates

Five-week-old female BALB/c mice were purchased and housed in the Animal Care Facilities in Seoul National University. BALB/c mice bearing subcutaneous tumors were used as an animal model for evaluation of the tissue distribution and anticancer activity of the chitosan/DOX/TAT conjugate. To measure the tissue distribution of the applied samples, including chitosan/Dox and chitosan/Dox/TAT, 50 μL samples were injected *via* peritumoral injection, followed by dissection of the tumor 12 h after injection. The optimum cutting temperature-mounted frozen sections were prepared and then examined with a confocal microscope. The serum was collected and its volume measured, followed by homogenization and measurement of fluorescence using a spectrophotometer. In addition, tissues including the liver, heart, spleen, kidney and lung were dissected, weighed and homogenized, and their fluorescence was measured using a spectrofluorometer (FP-6500; JASCO, Tokyo, Japan). The fluorescence was expressed as a percentage of injected dose per gram of tissue.

To generate tumors, 5-week-old BALB/c mice were subcutaneously injected in the right hind flank with 100 μL of a single-cell suspension containing 4×10^6 CT-26 cells. Tumor size was measured with Vernier calipers for the largest (length) and smallest (width) superficial visible diameters of the protruding tumor mass through the skin. Tumor volumes were calculated according to the following formula: volume = $0.52 \times W^2 \times L$, where W and L represent the width and length, respectively.²⁴ Treatment of the tumors was started 2 weeks after tumor implantation, when their size reached about 100–150 mm³. Test compounds included (i) PBS solution (control); (ii) DOX (100 μM); (iii) chitosan/DOX (100 μM); and (iv) chitosan/DOX/TAT conjugate (100 μM DOX equivalent). Each experimental group contained eight mice. The mice were treated (50 μL volume) nine times over 15 days *via* peritumoral injection. Tumor volumes were measured at 3–4-day intervals. At the end of the observation period, the mice were sacrificed and autopsied. The tumors were removed, weighed and fixed with formalin.

Statistical analysis

All measurements were conducted in triplicate and expressed as the mean ± standard deviation. The Student's *t* test was performed to compare the statistical significance of the *in vitro* cytotoxicity, *in vivo* antitumor effects and biodistribution; *p* values <0.05 were considered as statistically significant.

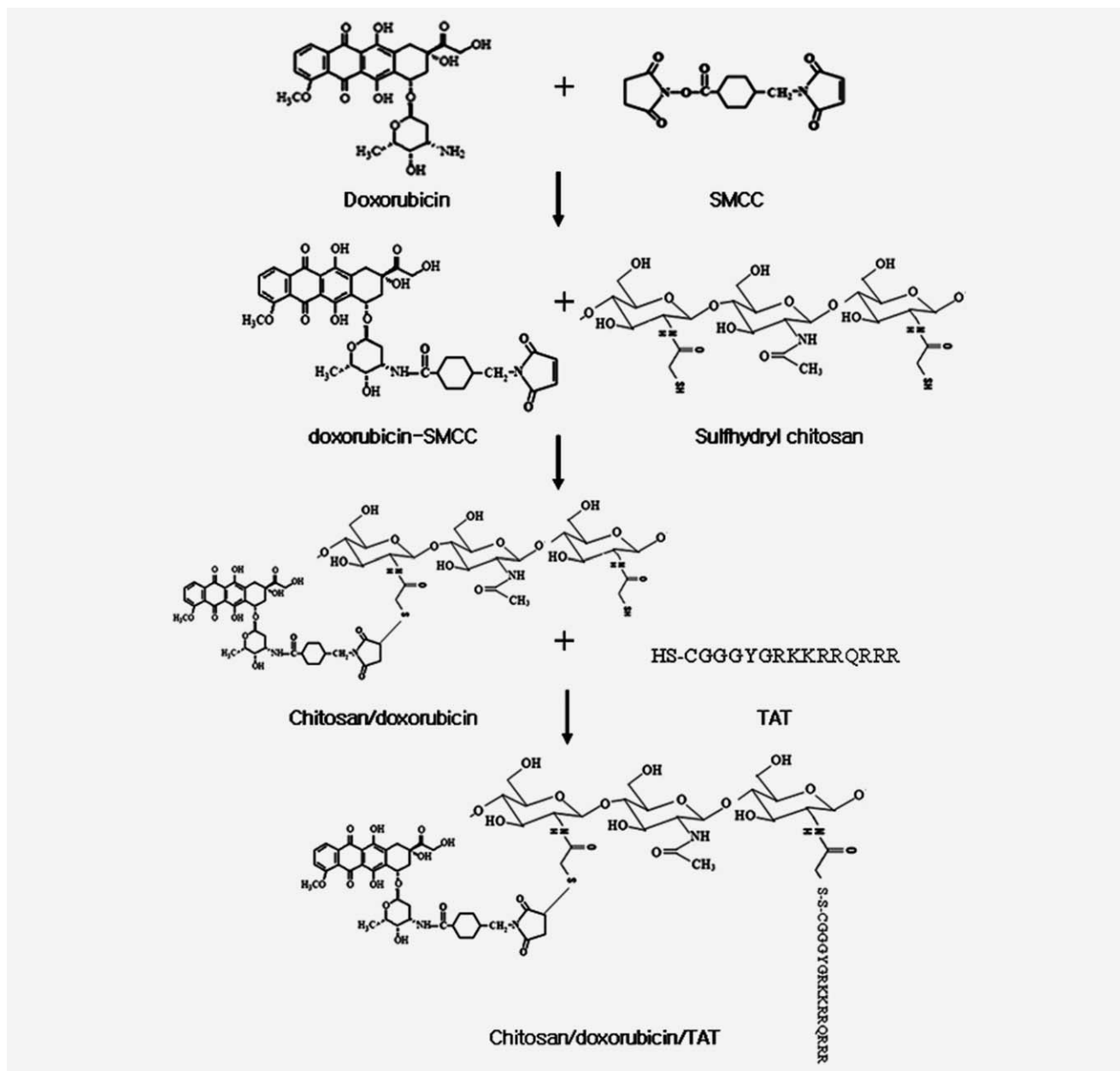


Figure 1. Scheme for the synthesis of the chitosan/DOX/TAT conjugate.

Results

Synthesis of chitosan/DOX/TAT

The reactive amino groups in the backbone of chitosan enable coupling with various bioactive molecules, including peptides and drugs, and antibodies.^{25–28} The scheme for chitosan/DOX/TAT conjugate synthesis is shown in Figure 1. The amino groups of chitosan were reacted with SATP to create a sulfhydryl group (-SH), followed by coupling with the SMCC-activated DOX. Chitosan/DOX conjugates were linked to a well-documented PTD, the TAT peptide, through the thiol group of the cysteine residue already introduced in the TAT peptide. Chitosan/DOX/TAT conjugates were formed through a stable disulfide bond. Because chitosan and DOX

were linked *via* noncleavable covalent bonds using the cross-linking agent SMCC, the conjugates were stable throughout the entire cell translocation process. The addition of the CGGG sequence between chitosan and the TAT peptide ensured the maximal maintenance of the cell-penetrating activity of TAT peptide. Unreacted doxorubicin, chitosan, TAT peptide, chitosan/DOX and chitosan/DOX/TAT conjugates were eluted from the heparin column *via* a linear elution using 2.0 M NaCl according to published methods.¹³ Peak III in Figure 2a had the same retention time as pure TAT peptide and, thus, was identified as unreacted TAT peptide. Collected peaks I to III were subjected to SDS-PAGE (Fig. 2b). Free doxorubicin was loaded in lane 1, and collected peaks I

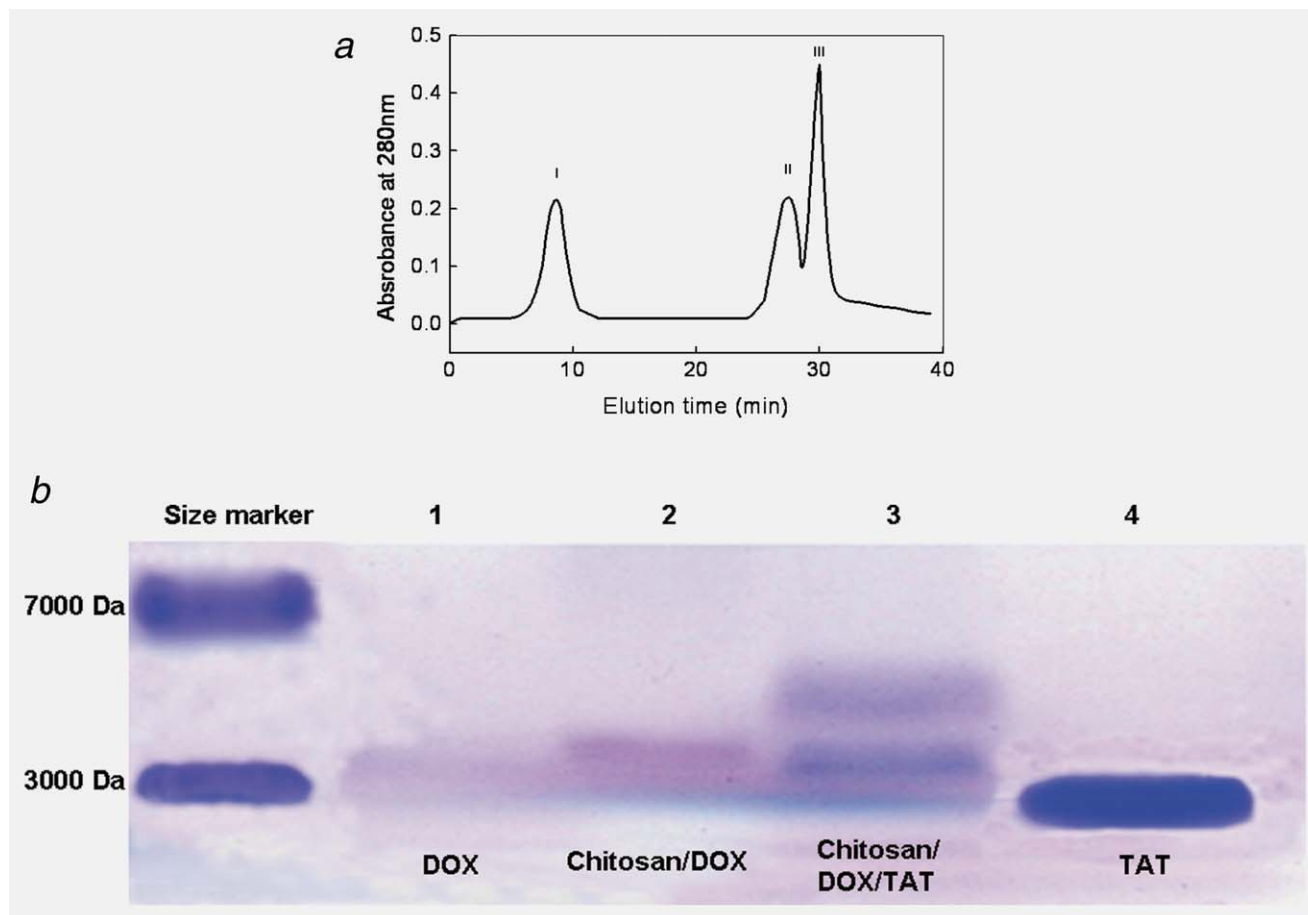


Figure 2. (a) Purification and characterization of chitosan/DOX/TAT conjugates by heparin affinity column chromatography; (b) SDS-polyacrylamide gel electrophoresis. Lanes 1, 2, 3 and 4 of the SDS-PAGE show DOX, chitosan/DOX, chitosan/DOX/TAT and free TAT, respectively. Electrophoresis images were obtained by Coomassie blue staining. [Color figure can be viewed in the online issue, which is available at wileyonlinelibrary.com.]

to III were loaded into lanes 2–4. The molecular weights of chitosan and TAT are 2,000 Da and 1,700 Da, respectively. Coomassie dyes bind to proteins through interactions with an arginine residue, aromatic amino acids and histidine.²⁹ The bands in lanes 1 (doxorubicin) and 2 (chitosan/DOX) were not stained strongly by Coomassie blue, but the band in lane 4 (TAT) was clearly stained. The molecular weight of the band in lane 3 (chitosan/DOX/TAT conjugates) was about 4,000 Da and was stained more clearly than the band in lane 2. The band in lane 3 thus demonstrated that chitosan/DOX/TAT conjugates were successfully linked.

Intracellular delivery of the chitosan/DOX conjugate is mediated by the TAT peptide

The cell permeability of the chitosan/DOX/TAT conjugate was compared with those of unconjugated DOX and the chitosan/DOX conjugate lacking the TAT peptide. As shown by the FACS results (Fig. 3a), during the 30-min incubation, the ability of chitosan/DOX/TAT to translocate was significant when compared to the conjugate lacking TAT and free dox-

orubicin. The free doxorubicin transduced into cells slightly better than did the chitosan/DOX conjugates.

The intracellular distribution pattern of the chitosan/DOX/TAT conjugate was observed by confocal microscopy (Fig. 3b). Although both free doxorubicin and the chitosan/DOX/TAT conjugate penetrated into CT-26 cells, different intracellular distributions were observed for these two compounds. The free DOX diffused only slightly into the cells, and the few internalized molecules accumulated in the nuclei due to their low molecular weight. In contrast, most of the chitosan/DOX/TAT conjugates displayed cytoplasmic localization as opposed to endosomal localization or simply adsorption onto the cell surface (Fig. 3b).

In vitro cytotoxic activity of the chitosan/DOX/TAT conjugates

The anticancer activity of the conjugates in the cells, *i.e.*, the cytotoxicity of the conjugate, was measured using chitosan/DOX, chitosan/DOX/TAT and free DOX in CT-26 colon adenocarcinoma cells in a log-phase culture (Fig. 4). The

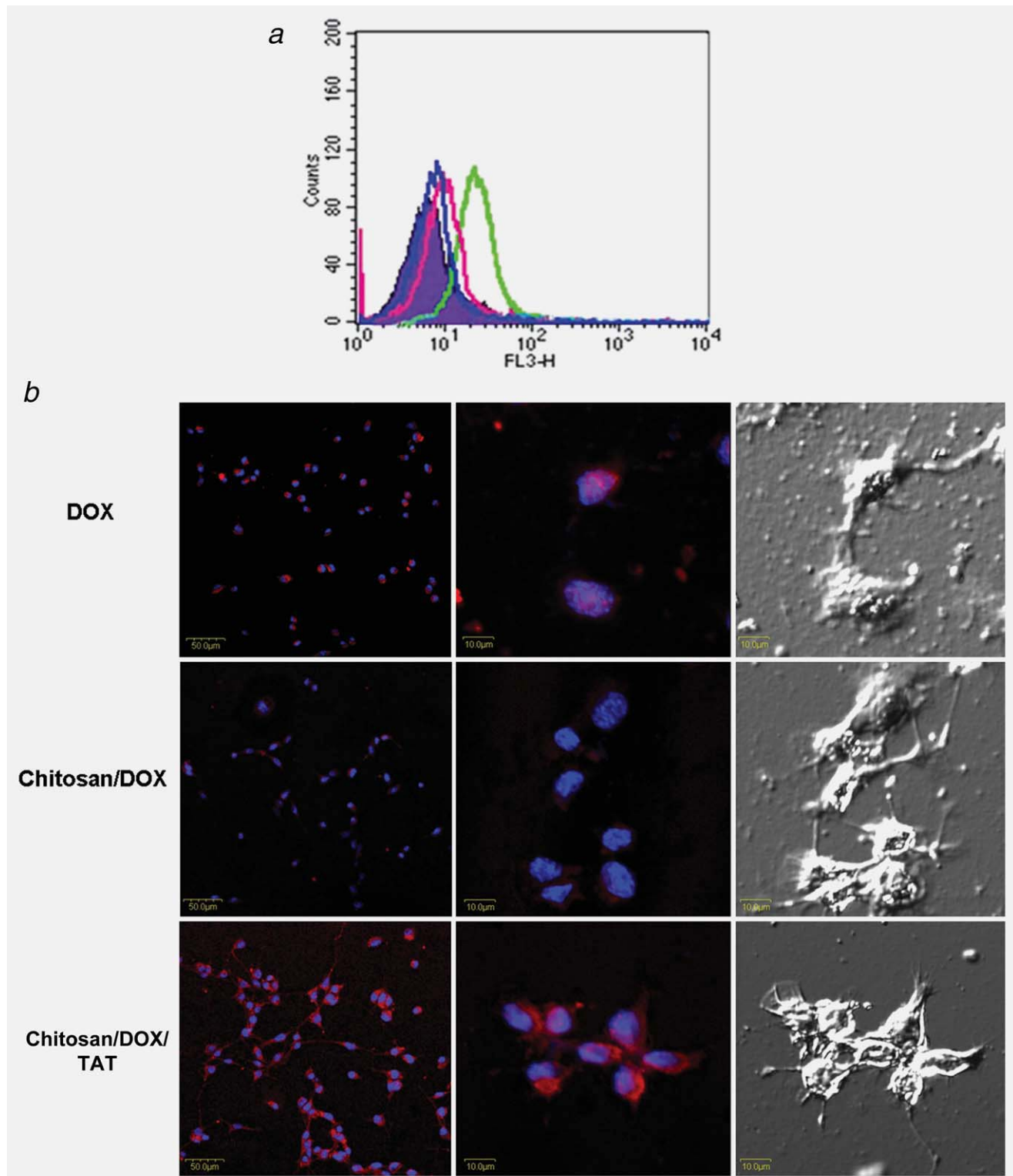


Figure 3. (a) FACS analysis of the cell uptake of DOX, chitosan/DOX and chitosan/DOX/TAT conjugates into the CT-26 cell line (1×10^6 cells/well). Control (purple peak) cells. DOX (red peak), chitosan/DOX (blue peak), chitosan/DOX/TAT (green peak) treated cells. Data obtained from triplicate experiments with at least four samples ($n = 4$). (b) Cellular localization of DOX, chitosan/DOX and chitosan/DOX/TAT in CT-26 adenocarcinoma cells. Cellular localization was monitored by confocal microscopy. The conjugates were visualized with DOX (orange), and the nucleus was visualized with Hoechst 33342 (blue). [Color figure can be viewed in the online issue, which is available at wileyonlinelibrary.com.]

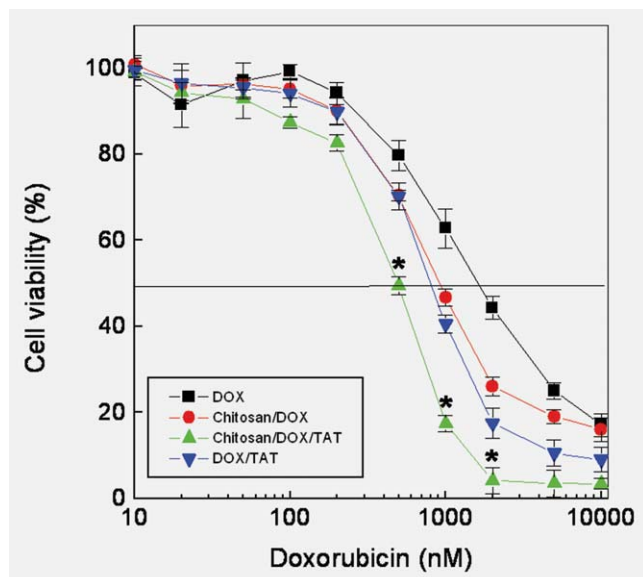


Figure 4. Cytotoxicity due to DOX (■), chitosan/DOX (●), chitosan/DOX/TAT (▲) and DOX/TAT (▼) in CT-26 colon adenocarcinoma cells in log-phase culture. The amount of cells remaining was assessed by an MTT assay and then compared with those of untreated cells in the control wells. Data obtained from triplicate experiments with at least four samples ($n = 4$) are presented as mean \pm SD. * $p < 0.05$, as compared to chitosan/DOX at the same concentration. [Color figure can be viewed in the online issue, which is available at wileyonlinelibrary.com.]

chitosan/DOX/TAT conjugate was much more potent than either the free DOX or the chitosan/DOX conjugate in killing CT-26 cells. The cytotoxicity of chitosan/DOX/TAT was significant at 500 nM ($p = 0.0013$), 1,000 nM ($p = 0.0004$) and 2,000 nM ($p = 0.0037$) compared to that of chitosan/DOX. The IC_{50} (inhibitory concentration 50%) value (as measured by the MTT assay) of the chitosan/DOX/TAT conjugate was approximately 480 nM, which was about 2 times less than that of chitosan/DOX (980 nM) and 4 times less than that of free DOX. In contrast, the IC_{50} of the chitosan/DOX conjugate (980 nM) was 1.5 times less than that of free doxorubicin. The IC_{50} of the DOX/TAT conjugate was 822 nM, which was higher than that of chitosan/DOX/TAT and lower than that of chitosan/DOX.

In vivo tumor regression activity of the chitosan/DOX/TAT conjugates

To confirm that the chitosan/DOX/TAT conjugates actually penetrate into tumors, the conjugates were applied *in vivo*. The tumor tissues from chitosan/DOX/TAT-treated mice displayed a strong and uniform red staining due to DOX on the conjugates (Fig. 5a). Conversely, mice injected with chitosan/DOX displayed a sporadic and weak staining of DOX (Fig. 5b). The fluorescence in other organs, including the liver, heart, spleen, kidney, lung and serum, were examined for the possibility of nonspecific distribution of chitosan/DOX conjugates. The conjugates of chitosan/DOX/TAT displayed higher fluorescence in

the tumor, followed by the kidney (Fig. 5c). The uptake of chitosan/DOX/TAT in the tumor ($p = 0.0013$) was significantly higher than that of chitosan/DOX conjugate; however, it decreased in the kidney ($p = 0.0122$) and liver ($p = 0.0073$).

To assay the biological consequences of treating subcutaneous solid tumors with chitosan/DOX/TAT, conjugates were injected into the peritoneal cavities of test samples (Fig. 6). Pooled data from multiple experiments revealed that treatment with chitosan/DOX/TAT resulted in a substantial reduction in tumor mass in all mice. In comparison, tumors treated with free DOX or chitosan/DOX were larger than their TAT-conjugated counterparts in all mice. As can be seen, tumors continued to grow in control mice injected with PBS solution, and the average volume of the excised tumors reached from 1,200 to 7,500 mm² during 2 weeks and 4 weeks of treatment. In contrast, tumor growth in the mice treated with chitosan/DOX/TAT conjugate showed considerable regression and significantly reduced to 900 mm² (range between 600 and 1,900 mm²).

Tumor volume following treatment with the chitosan/DOX/TAT conjugate showed a significant decrease at 20 days ($p = 0.0037$), 24 days ($p = 0.0242$), 27 days ($p = 0.0031$) and 30 days ($p = 0.0127$) compared to tumor volume following treatment with the chitosan/DOX conjugate.

Discussion

Drug therapies, especially anticancer drug therapies, are hindered by two major obstacles. One obstacle is the lack of preferential target cell killing, whereas the other is the poor translocation through cell membranes. The first hurdle can be overcome by applying a combination of prodrug and targeting approaches using antibodies.^{30–32} To resolve the second limitation, the most established method is to use receptor-mediated endocytosis or phagocytosis,³³ despite serious setbacks such as low uptake efficiency³⁴ and the need for drug release from endosome.³⁵ At present, few delivery systems are capable of overcoming these two limitations, and none of them provides evidence of macromolecular drug delivery such as proteins or genetic materials. Therefore, a highly effective delivery system, particularly for hydrophilic, macromolecular drug types, is imperative, and the quest remains. In this regard, PTDs or cell-penetrating peptides, corresponding to short 30-residue synthetic peptides, are the most promising strategy to overcome both extracellular and intracellular limitations to the administration of various biomolecules, including proteins,³⁵ polymeric drugs³⁶ and even solid nanoparticles.⁸

The polymer-drug conjugate exhibits decreased clearance and prolonged circulation, thereby providing sufficient time for the polymer-drug conjugate to accumulate at the target site and precluding the undesirable side effects generated by free drug.³⁷ However, macromolecular drug delivery systems are internalized by the cells through endocytosis, which might impede trafficking to subcellular targets.⁴ Therefore, PTDs have been applied to aid internalization of macromolecular drug

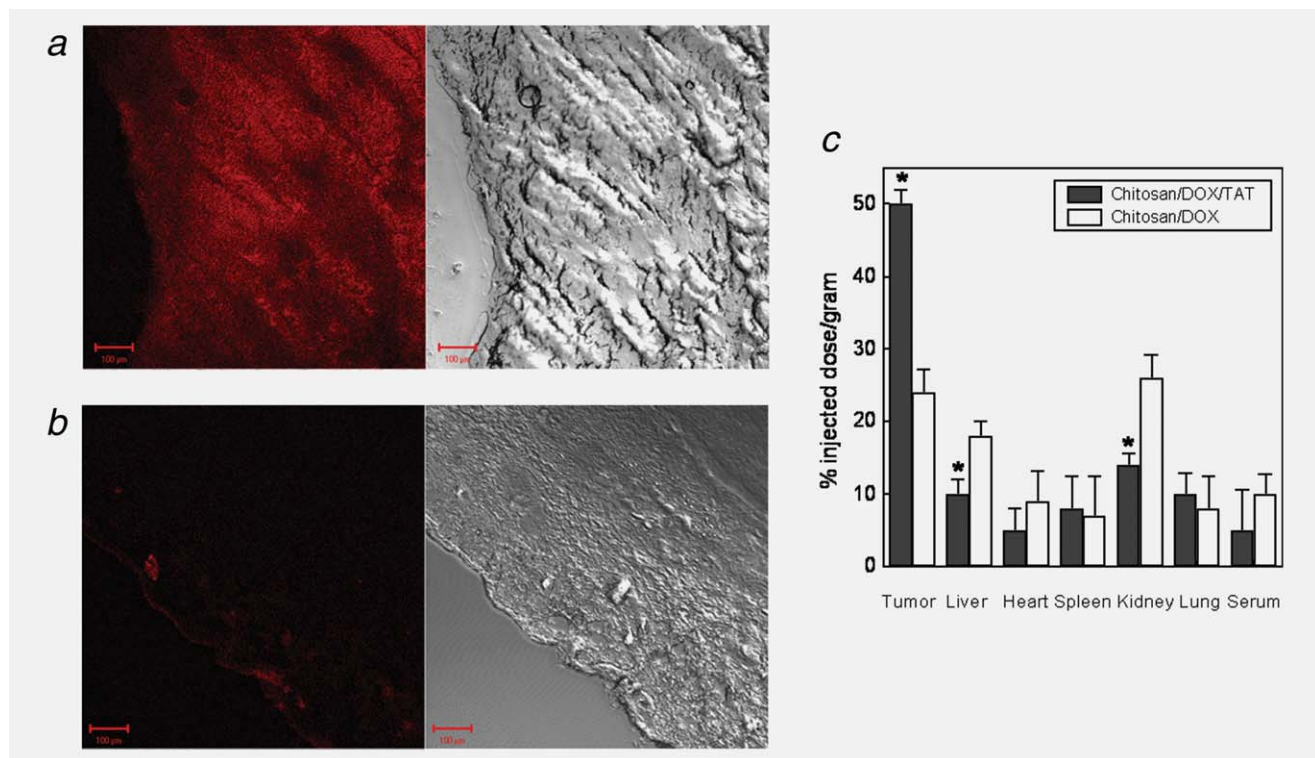


Figure 5. Tumor distribution into the colon cancer of (a) chitosan/DOX/TAT and (b) chitosan/DOX. The left panel indicates the fluorescent image of the conjugate in the tumor tissues, whereas the right panel was an identical DIC mode picture. (c) The organ distribution of the chitosan/DOX/TAT conjugate and chitosan/DOX measured at 12 h after injection. * $p < 0.05$, as compared to chitosan/DOX in the same organ. [Color figure can be viewed in the online issue, which is available at wileyonlinelibrary.com.]

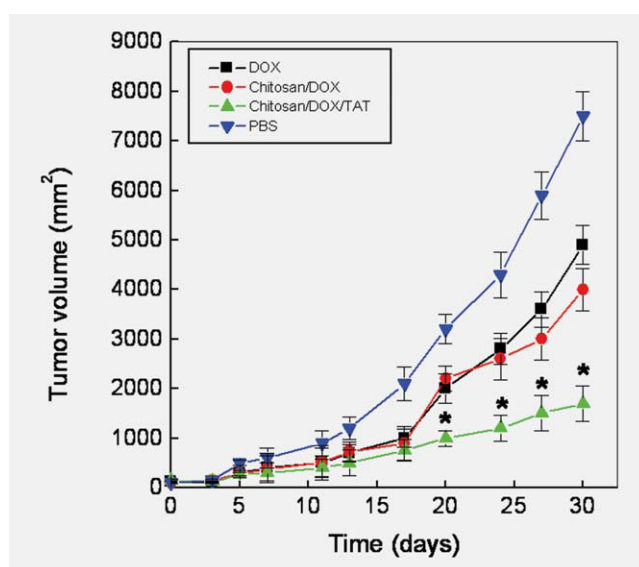


Figure 6. Tumor volume was determined by caliper measurements taken twice per week and averaged for each treatment group (see Materials and Methods section). DOX (■), chitosan/DOX (●), chitosan/DOX/TAT (▲) and PBS (▼). * $p < 0.05$, as compared to chitosan/DOX at the same time. [Color figure can be viewed in the online issue, which is available at wileyonlinelibrary.com.]

conjugates. Herein, the authors applied TAT peptides as the PTD for the internalization of chitosan/DOX conjugates. The translocation and intracellular distribution patterns of chitosan/DOX/TAT into cells were demonstrated by FACS and confocal microscopy, respectively (Figs. 3 and 4). The translocation of chitosan/DOX/TAT was significant when compared to the conjugate lacking TAT and free DOX. The free DOX transduced into cells slightly better than did the chitosan/DOX conjugates. Different intracellular distributions were observed for both free DOX and the chitosan/DOX/TAT conjugate, although both free DOX and the chitosan/DOX/TAT conjugate penetrated into CT-26 cells (Fig. 4). The chitosan/DOX conjugates were not transduced into the cytosol due to their increased molecular weight. It has been shown that positively charged polymers, such as chitosan and polylysine, are transduced into cells *via* adsorption-mediated endocytosis,³⁸ which is in agreement with our current results regarding the distribution of chitosan/DOX conjugates. The conjugates with TAT attached, however, demonstrated a cytoplasmic distribution rather than an endoplasmic retention. From the enhanced distribution of these molecules in the tumor tissues, we expected an increased antitumor effect from the chitosan/DOX/TAT conjugates. Almost all of the chitosan/DOX/TAT conjugates were found inside the cell, specifically in the cytosol of the CT-26 cells (Fig. 4). In agreement with results previously reported for TAT- or other PTD-

linked protein conjugates,^{39,40} further incubation of the cells with the TAT conjugate resulted in the localization of the conjugates into the nucleus (data not shown).

The chitosan/DOX/TAT conjugate was much more effective than the free DOX, chitosan/DOX conjugate or DOX/TAT conjugates in killing CT-26 cells (Fig. 5). The anticancer activity of chitosan/DOX/TAT demonstrated that the covalent linking to TAT was able to successfully transduce otherwise endocytosable polymeric drugs into cancer cells for potential therapeutic purposes. This rapid intracellular transduction of chitosan/DOX/TAT was able to cause significant cytotoxic effects in CT-26 cells, as demonstrated by a much lower IC₅₀ value. In a previous study, DOX/TAT conjugates were more potent in killing drug resistant MCF-7 cells than free DOX.¹¹ In this study, the IC₅₀ of chitosan/DOX/TAT was 480 nM, the IC₅₀ of DOX/TAT was 820 nM and the IC₅₀ of chitosan/DOX was 980 nM. The introduction of TAT to free DOX makes it more cytotoxic than attaching chitosan to free DOX. When both chitosan and TAT were conjugated to free DOX, there was a significant IC₅₀ lowering effect. In a previous study, the TAT-protein conjugate had a considerably lower IC₅₀ concentration than did that of the antibody-protein conjugate that mediates endocytosis.^{13,41,42} The superior cytotoxicity of the chitosan/DOX/TAT conjugate was apparently due to the increased cell-internalization efficiency of TAT, overcoming the endocytic machinery of the cell and also overcoming the increased retention time in cells by the EPR effect of chitosan. Concerning the EPR effect, attempts have been made to generate polymeric carriers in combination with small and free anticancer drugs with some success. Eliaz *et al.*⁴³ reported that doxorubicin encapsulated in targeted liposomes was more efficient in killing murine melanoma cells than was free doxorubicin. They reported that kinetic profile of antitumor toxicity by the free DOX reached noticeable regression of tumor cells 96 h after the treatment, which maintained similar extent of toxicity level (*i.e.*, % cell survival). In comparison, liposome with DOX loading was faster than free DOX to reach the noticeable tumor cell regression, as similar regression of cell survival by the liposomal DOX was obtained 12 h after the treatment. Liposome carrier has difference in the payloads of active drug, *i.e.*, 1 unit of liposomal carrier presents much higher DOX equivalence than free DOX, providing faster tumor killing activity. Polymeric carrier also possesses similar characteristics to liposome carrier in terms of high drug loading. Therefore, based on this report,⁴³ polymeric DOX was anticipated to follow similar kinetics to liposome and present marked cytotoxicity.

In our study, chitosan/DOX/TAT conjugates penetrated into the cells within 30 min, as demonstrated by FACS analysis and confocal microscope observation. Although the author performed the cytotoxicity test for 1 day, the chitosan/DOX/TAT conjugates might affect the cell cytotoxicity regardless of the culture period. In addition, the tumor distribution also clearly indicated the fast translocalization of the chitosan/DOX/TAT conjugate in the tumor compared to the chitosan/DOX over 12 h (Fig. 6). Although the chitosan/DOX conjugate by itself could

create an EPR effect, the slow distribution to the tumor with increased kidney, liver, heart and serum uptake demonstrated a less effective antitumor activity compared to that with the TAT conjugate. Therefore, *in vitro* cytotoxicity and *in vivo* antitumor activity of both conjugates demonstrated different results.

The subcutaneous tumor mass was substantially reduced by treatment with chitosan/DOX/TAT conjugates compared to treatment with free DOX or chitosan/DOX. It is probable that the efficiency in tumor regression could be partly due to the high cytosolic localization of the TAT-linked chitosan/DOX, which was then able to exert its maximum antitumor effects. The antitumor effect of chitosan/DOX/TAT resulted from the significantly enhanced concentration of the chitosan/DOX/TAT conjugates in the tumor tissue over other organs (Fig. 7).

In vivo tumor regression result by the treatment using chitosan/DOX/TAT was far more convincing than by *in vitro* cellular IC₅₀ results, which already provided evidence of conjugate the anticancer activity by the same conjugate. The *in vitro* cytotoxicity was primarily due to the hydrolyzed DOX from the backbone of chitosan and chitosan/TAT. A small molecular drug such as DOX is able to penetrate a single cell layer, as confirmed by confocal observation. The cellular cytotoxicity was not highly influenced by the presence of TAT in the backbone of chitosan. However, *in vivo* conditions recruited dense tumor tissue, which was hard to penetrate compared to the single cell membrane; therefore, the TAT could exert its own penetrating capacity in the *in vivo* condition, demonstrating a marked antitumor result as compared with that obtained in the *in vitro* study. The tumor penetration capacity of PTD conjugates has been previously reported by the authors.¹³ The *in vitro* transduction results determined for the chitosan/DOX/TAT conjugate and the *in vivo* tumor regression induced by the conjugate suggest TAT-mediated transduction. The TAT-mediated, chitosan-based approach offers significant advantages over the antibody- or other receptor-based delivery systems for the delivery of small drugs. Indeed, this chitosan system inherits all of the advantages of polymer-based systems for delivering small drugs, such as high drug loading and stabilizing effects.^{4,6,15} Yet, this system is still able to achieve active drug targeting and superefficient cellular drug uptake, in contrast to the slow uptake encountered with particulate-based delivery systems. In addition, the hydrophilic nature of TAT and chitosan could render hydrophobic drugs more soluble and bioavailable, whereas the ability of TAT to transport all drug types could render membrane-impermeable hydrophilic drugs cytotoxic. Moreover, the polymeric architecture of the chitosan-based system delivers high drug payloads, thereby increasing the cytotoxic activity for the same drug concentration. Because the conjugate displays rapid cell uptake, the findings of this study open up possibilities for the treatment of cancers. In summary, both the *in vitro* and *in vivo* results demonstrate that TAT-conjugated chitosan/DOX is potent in regressing tumor growth and might be a powerful tool for anticancer drug development.

References

- Malugin A, Kopeckova P, Kopecek J. HPMA copolymer-bound doxorubicin induces apoptosis in human ovarian carcinoma cells by a Fas-independent pathway. *Mol Pharm* 2004;1:174–82.
- Malugin A, Kopeckova P, Kopecek J. HPMA copolymer-bound doxorubicin induces apoptosis in ovarian carcinoma cells by the disruption of mitochondrial function. *Mol Pharm* 2006;3:351–61.
- Cheng J, Khin KT, Davis ME. Antitumor activity of beta-cyclodextrin polymer-camptothecin conjugates. *Mol Pharm* 2004;1:183–93.
- Kopecek J, Kopeckova P, Minko T, Lu Z. HPMA copolymer-anticancer drug conjugates: design, activity, and mechanism of action. *Eur J Pharm Biopharm* 2000;50:61–81.
- Maeda H, Seymour LW, Miyamoto Y. Conjugates of anticancer agents and polymers: advantages of macromolecular therapeutics in vivo. *Bioconjug Chem* 1992;3:351–62.
- Duncan R. Drug-polymer conjugates: potential for improved chemotherapy. *Anticancer Drugs* 1992;3:175–210.
- Kang H, DeLong R, Fisher MH, Juliano RL. Tat-conjugated PAMAM dendrimers as delivery agents for antisense and siRNA oligonucleotides. *Pharm Res* 2005;22:2099–106.
- Lewin M, Carlesso N, Tung CH, Tang XW, Cory D, Scadden DT, Weissleder R. Tat peptide-derivatized magnetic nanoparticles allow in vivo tracking and recovery of progenitor cells. *Nat Biotechnol* 2000;18:410–4.
- Schwarze SR, Ho A, Vocero-Akbani A, Dowdy SF. In vivo protein transduction: delivery of a biologically active protein into the mouse. *Science* 1999;285:1569–72.
- Liu L, Venkatraman SS, Yang YY, Guo K, Lu J, He B, Moochhala S, Kan L. Polymeric micelles anchored with TAT for delivery of antibiotics across the blood-brain barrier. *Biopolymers* 2008;90:617–23.
- Liang JF, Yang VC. Synthesis of doxorubicin-peptide conjugate with multidrug resistant tumor cell killing activity. *Bioorg Med Chem Lett* 2005;15:5071–5.
- Liang JF, Yang VC. Insulin-cell penetrating peptide hybrids with improved intestinal absorption efficiency. *Biochem Biophys Res Commun* 2005;335:734–8.
- Park YJ, Chang LC, Liang JF, Moon C, Chung CP, Yang VC. Nontoxic membrane translocation peptide from protamine, low molecular weight protamine (LMWP), for enhanced intracellular protein delivery: in vitro and in vivo study. *Faseb J* 2005;19:1555–7.
- Lee KY, Kim JH, Kwon IC, Jeong SY. Self-aggregates of deoxycholic acid modified chitosan as a novel carrier of adriamycin. *Colloid Polym Sci* 2000;278:1216–9.
- Ruel-Gariepy E, Leclair G, Hildgen P, Gupta A, Leroux JC. Thermosensitive chitosan-based hydrogel containing liposomes for the delivery of hydrophilic molecules. *J Control Release* 2002;82:373–83.
- Kim YH, Gihm SH, Park CR, Lee KY, Kim TW, Kwon IC, Chung H, Jeong SY. Structural characteristics of size-controlled self-aggregates of deoxycholic acid-modified chitosan and their application as a DNA delivery carrier. *Bioconjug Chem* 2001;12:932–8.
- Koping-Hoggard M, Tubulekas I, Guan H, Edwards K, Nilsson M, Varum KM, Artursson P. Chitosan as a nonviral gene delivery system. Structure-property relationships and characteristics compared with polyethylenimine in vitro and after lung administration in vivo. *Gene Ther* 2001;8:1108–21.
- Roy K, Mao HQ, Huang SK, Leong KW. Oral gene delivery with chitosan—DNA nanoparticles generates immunologic protection in a murine model of peanut allergy. *Nat Med* 1999;5:387–91.
- Dufes C, Schatzlein AG, Tettley L, Gray AI, Watson DG, Olivier JC, Couet W, Uchegbu IF. Niosomes and polymeric chitosan based vesicles bearing transferrin and glucose ligands for drug targeting. *Pharm Res* 2000;17:1250–8.
- Park YJ, Kim KH, Lee JY, Ku Y, Lee SJ, Min BM, Chung CP. Immobilization of bone morphogenetic protein-2 on a nanofibrous chitosan membrane for enhanced guided bone regeneration. *Biotechnol Appl Biochem* 2006;43:17–24.
- Bally MB, Nayar R, Masin D, Cullis PR, Mayer LD. Studies on the myelosuppressive activity of doxorubicin entrapped in liposomes. *Cancer Chemother Pharmacol* 1990;27:13–9.
- Mitra S, Gaur U, Ghosh PC, Maitra AN. Tumor targeted delivery of encapsulated dextran-doxorubicin conjugate using chitosan nanoparticles as carrier. *J Control Release* 2001;74:317–23.
- Chang LC, Lee HF, Yang Z, Yang VC. Low molecular weight protamine (LMWP) as nontoxic heparin/low molecular weight heparin antidote (I): preparation and characterization. *AAPS PharmSci* 2001;3:E17.
- Arbiser JL, Moses MA, Fernandez CA, Ghiso N, Cao Y, Klauber N, Frank D, Brownlee M, Flynn E, Parangi S, Byers HR, Folkman J. Oncogenic H-ras stimulates tumor angiogenesis by two distinct pathways. *Proc Natl Acad Sci U S A* 1997;94:861–6.
- Aoki T, Iskandar S, Yoshida T, Takahashi K, Hattori M. Reduced immunogenicity of beta-lactoglobulin by conjugating with chitosan. *Biosci Biotechnol Biochem* 2006;70:2349–56.
- Hyung Park J, Kwon S, Lee M, Chung H, Kim JH, Kim YS, Park RW, Kim IS, Bong Seo S, Kwon IC, Young Jeong S. Self-assembled nanoparticles based on glycol chitosan bearing hydrophobic moieties as carriers for doxorubicin: in vivo biodistribution and anti-tumor activity. *Biomaterials* 2006;27:119–26.
- Lee JY, Choo JE, Choi YS, Shim IK, Lee SJ, Seol YJ, Chung CP, Park YJ. Effect of immobilized cell-binding peptides on chitosan membranes for osteoblastic differentiation of mesenchymal stem cells. *Biotechnol Appl Biochem* 2009;52:69–77.
- Yoo HS, Lee JE, Chung H, Kwon IC, Jeong SY. Self-assembled nanoparticles containing hydrophobically modified glycol chitosan for gene delivery. *J Control Release* 2005;103:235–43.
- Westermeier R, Gronau S. Electrophoresis in practice : a guide to methods and applications of DNA and protein separations. 4th Rev. Weinheim: Wiley-VCH, 2005.
- Liang JF, Li YT, Song H, Park YJ, Naik SS, Yang VC. ATTEMPTS: a heparin/protamine-based delivery system for enzyme drugs. *J Control Release* 2002;78:67–79.
- Syrigos KN, Epenetos AA. Antibody directed enzyme prodrug therapy (ADEPT): a review of the experimental and clinical considerations. *Anticancer Res* 1999;19:605–13.
- Chari RV. Targeted delivery of chemotherapeutics: tumor-activated prodrug therapy. *Adv Drug Deliv Rev* 1998;31:89–104.
- Mellman I. Endocytosis and molecular sorting. *Annu Rev Cell Dev Biol* 1996;12:575–625.
- Niesner U, Halin C, Lozzi L, Gunthert M, Neri P, Wunderli-Allenspach H, Zardi L, Neri D. Quantitation of the tumor-targeting properties of antibody fragments conjugated to cell-permeating HIV-1 TAT peptides. *Bioconjug Chem* 2002;13:729–36.
- Fawell S, Seery J, Daikh Y, Moore C, Chen LL, Pepinsky B, Barsoum J. Tat-mediated delivery of heterologous proteins into cells. *Proc Natl Acad Sci U S A* 1994;91:664–8.
- Moon C, Kwon YM, Lee WK, Park YJ, Chang LC, Yang VC. A novel polyrotaxane-based intracellular delivery

- system for camptothecin: in vitro feasibility evaluation. *J Biomed Mater Res A* 2008;84: 238–46.
37. Nori A, Kopecek J. Intracellular targeting of polymer-bound drugs for cancer chemotherapy. *Adv Drug Deliv Rev* 2005; 57:609–36.
38. Wagner E, Ogris M, Zauner W. Polylysine-based transfection systems utilizing receptor-mediated delivery. *Adv Drug Deliv Rev* 1998;30:97–113.
39. Morris MC, Depollier J, Mery J, Heitz F, Divita G. A peptide carrier for the delivery of biologically active proteins into mammalian cells. *Nat Biotechnol* 2001;19: 1173–6.
40. Becker-Hapak M, McAllister SS, Dowdy SF. TAT-mediated protein transduction into mammalian cells. *Methods* 2001;24: 247–56.
41. McGrath MS, Rosenblum MG, Philips MR, Scheinberg DA. Immunotoxin resistance in multidrug resistant cells. *Cancer Res* 2003; 63:72–9.
42. Rosenblum MG, Shawver LK, Marks JW, Brink J, Cheung L, Langton-Webster B. Recombinant immunotoxins directed against the c-erb-2/HER2/neu oncogene product: in vitro cytotoxicity, pharmacokinetics, and in vivo efficacy studies in xenograft models. *Clin Cancer Res* 1999;5: 865–74.
43. Eliaz RE, Nir S, Marty C, Szoka FC Jr. Determination and modeling of kinetics of cancer cell killing by doxorubicin and doxorubicin encapsulated in targeted liposomes. *Cancer Res* 2004;64: 711–8.